Lung Cancer 135 (2019) 56–65

Contents lists available at ScienceDirect

Lung Cancer

journal homepage: www.elsevier.com/locate/lungcan

Analysis of CCDC6 as a novel biomarker for the clinical use of PARP1 inhibitors in malignant pleural mesothelioma

Francesco Morra[a], Francesco Merolla[b,c], Debora D'Abbiero[a], Gennaro Ilardi[c], Severo Campione[d], Roberto Monaco[d], Gianluca Guggino[e], Francesca Ambrosio[f], Stefania Staibano[c], Aniello Cerrato[a], Roberta Visconti[a], Angela Celetti[a,*]

[a] Institute for the Experimental Endocrinology and Oncology, National Research Council, Naples, Italy
[b] Department of Medicine and Health Sciences "V. Tiberio", University of Molise, Campobasso, Italy
[c] Department of Advanced Biomedical Sciences, University "Federico II", Naples, Italy
[d] Pathology Unit, A. Cardarelli Hospital, Naples, Italy
[e] Thoracic Surgery Unit, A. Cardarelli Hospital, Naples, Italy
[f] Oncology Unit, A. Cardarelli Hospital, Naples, Italy

ARTICLE INFO

Keywords:
DNA repair
Homologous recombination
BAP1
USP7
P5091
Targeted therapy

ABSTRACT

Objectives: CCDC6 (coiled-coil domain containing 6) is a player of the HR response to DNA damage and has been predicted to interact with BAP1, another HR-DNA repair gene highly mutated in Malignant Pleural Mesothelioma (MPM), an aggressive cancer with poor prognosis. CCDC6 levels are modulated by the deubiquitinase USP7, and CCDC6 defects have been reported in several tumors determining PARP-inhibitors sensitivity. Our aim was to investigate the functional role of CCDC6 in MPM carcinogenesis and response to PARP-inhibitors.

Materials and Methods: The interaction between CCDC6 and BAP1 was confirmed in MPM cells, by co-immunoprecipitation. Upon USP7 inhibition, that induces CCDC6 degradation, the ability to repair the DSBs and the sensitivity to PARP inhibitors, was explored by HR reporter and by cells viability assays, respectively. A TMA including 34 MPM cores was immunostained for CCDC6, USP7 and BAP1 and the results correlated by statistical analysis.

Results: MPM cells depleted of CCDC6 showed defects in DSBs repair and sensitivity to PARP inhibitors. The silencing of CCDC6 when combined with the overexpression of BAP1-mutant (Δ221-238) enhanced the HR-DNA repair defects and the PARP inhibitors sensitivity.

In the TMA of MPM primary samples, the staining of CCDC6 and of its de-ubiquitinase USP7 showed a significant correlation in the tested primary samples ($p = 0.01$). CCDC6 was barely detected in 30% of the tumors that also carried BAP1 defects.

Conclusion: The combination of CCDC6 and BAP1 staining may indicate therapeutic options for DDR targeting, acting in synergism with cisplatinum.

1. Introduction

Malignant Pleural Mesothelioma (MPM) is an aggressive tumor that arises from the mesothelial cells of the pleura [1]. It is well established that MPM is almost always caused by professional or non professional exposure to asbestos fibers, while the pathogenetic role of cofactors, such as SV40 viral infection, still remains controversial [2,3]. The average latency period between asbestos exposure and tumor presentation is 30–45 years, depending on duration or intensity of exposure and patient gender [4]. Legislation banning asbestos has been adopted only about 50 years ago by just few countries, and the MPM worldwide incidence is still rising [5]. The precise biological mechanisms by which asbestos causes MPM are still debated, although a key role has been ascribed to chronic inflammation induced by asbestos

Abbreviations: MPM, Malignant pleural mesothelioma; CCDC6, coiled coil domain containing 6; PARP, Poly (ADP-ribose) polymerase; DDR, DNA damage response; DSBs, double strand breaks; HR, homologous recombination; CI, combination index; TMA, tissue micro array; H&E, hematoxylin and eosin stain; IHC, immunohistochemistry

* Corresponding author.
E-mail address: celetti@unina.it (A. Celetti).

https://doi.org/10.1016/j.lungcan.2019.07.011
Received 15 April 2019; Received in revised form 22 June 2019; Accepted 12 July 2019

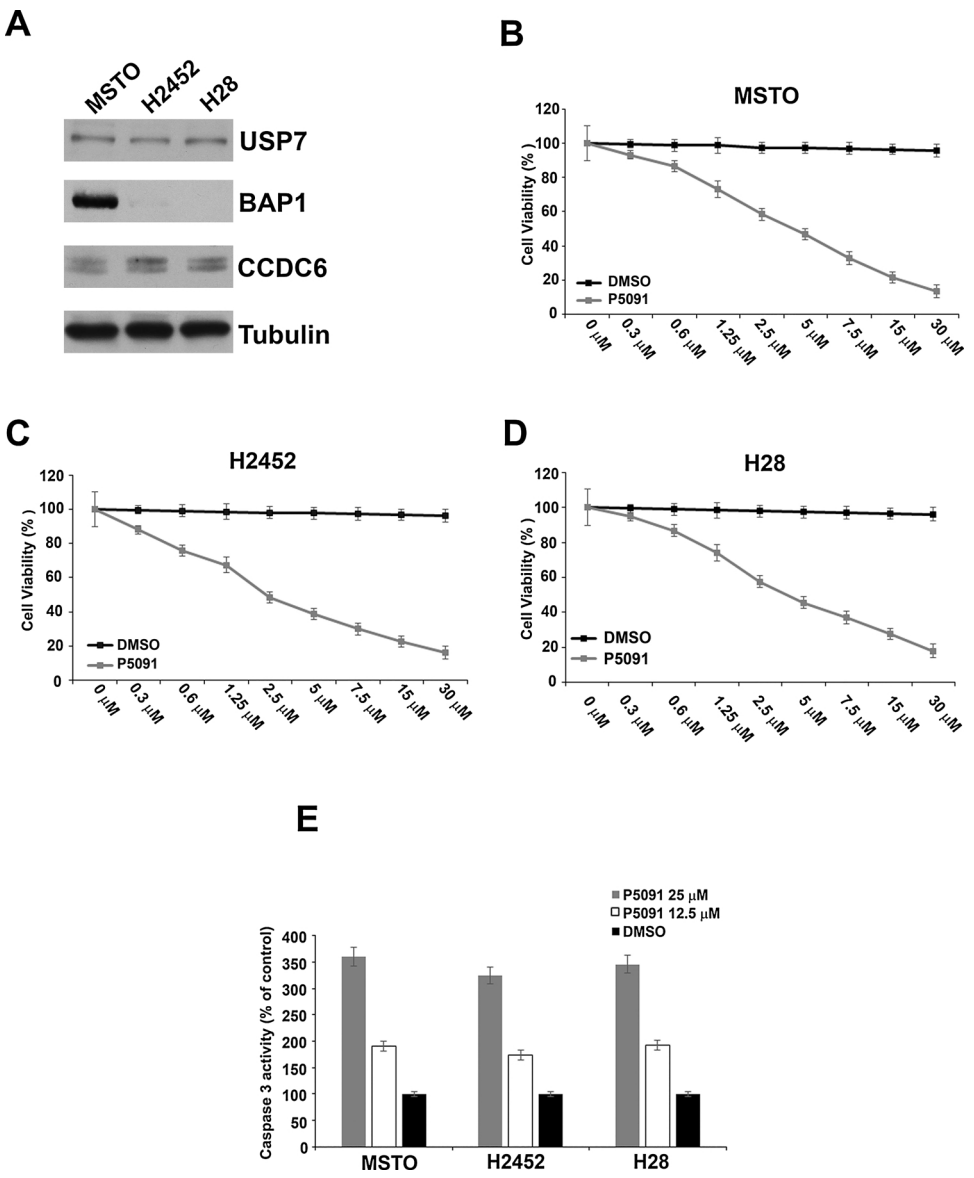

Fig. 1. CCDC6 levels in mesothelioma cell lines can be modulated by the USP7 inhibitor P5091 (A) Immunoblot analysis of USP7, BAP1 and CCDC6 in human MPM cell lines MSTO-H211, H2452 and H28. Anti-tubulin is shown as loading control. Surviving fractions of MSTO-H211 (B), H2452 (C) and H28 (D) cells are shown. Cells were seeded in 96-well plates and 24 h later exposed to vehicle (DMSO) or P5091 at the indicated doses for 144 h and analysed for viability using a modified 3-(4,5-dimethylthiazole-2-yl)-2-5-duphenyltetrazolium bromide assay, CellTiter 96 Aqueous one Solution assay (Promega). The values are presented as mean standard deviation of three independent experiments. (E) Caspase 3 activity was evaluated in the MSTO-H211, H2452 and H28 cells treated or not treated with P5091 for 24 h, as indicated. The plotted values represent the mean +/- s.e.m. of three independent experiments.

fibers [6,7]. Inflammatory microenvironment might promote tumor cell proliferation and survival, support angiogenesis and invasion, and cause tumor immune escape [1,8].

Currently, the only FDA-approved chemotherapy treatment for MPM is cisplatin plus pemetrexed, with few selected patients responsive to multimodal therapy including cytoreductive surgery, chemo- and radiotherapy [9,10]. However, MPM is highly refractory to treatment, and patients survive 12 months on average with standard therapy [11]. The only recent major advance in MPM treatment is the discovery of the monoclonal antibody bevacizumab that improves the patient's overall survival preventing tumor neoangiogenesis by blocking the VEGF binding [12]. Comprehensive genomic analyses of MPM have been performed to identify specific genetic alterations to target. The tumor suppressors CDKN2A, NF2 and BAP1 are often inactivated [13–16]. Of note, BAP1 germline mutations are responsible for a rare syndrome predisposing to cancer including pleural mesothelioma [17,18]. Overall, it has been estimated that homozygous inactivating mutations of BAP1 are present in about 50% of MPMs [19]. BAP1 gene encodes for a deubiquitinating enzyme, phosphorylated by ATM, that is required for an efficient assembly of the homologous recombination (HR) complex including BRCA1 and RAD51 upon induced DNA double strand breaks (DSBs) by genotoxic stress [20,21]. BAP1 loss-of-function mutations have been described as sensitizing cancer cells to either ionizing or ultraviolet radiation, to asbestos, and to poly(adenosine diphosphate–ribose) polymerase (PARP) inhibition [22], indicating a role of functional BAP1 in promoting DSBs repair. Accordingly, BAP1 germline and somatic mutations impair DSBs repair and cell recovery from DNA damage [23,24].

DSBs are the most dangerous form of DNA damage: unrepaired breaks can cause cell death, and an inaccurate repair can result in chromosome translocations or mutations that can lead to malignant transformation. The eukaryotic cells have evolved three different pathways to repair DSBs, the HR being the most conservative one [25].

The CCDC6 protein is a substrate of ATM and is a player of the HR response to DNA damage [26]. CCDC6 is a negative regulator of the serin-threonin Protein Phosphatase 4c (PP4c) that dephosphorylates γH2AX, an efficient coordinator of the DNA repairing process [27]. The loss of function of CCDC6 results in PP4c-induced γH2AX dephosphorylation and, in turn, in an inappropriate resolution of DNA repairing process [28]. In absence of CCDC6, the cells repair the DSBs by a non homologous-end-joining mechanism that is more prone than HR mechanisms to generate errors, as well as it occurs in the BRCA defective cells. The impairment of CCDC6 function occurs by different mechanisms in many human cancers [29]. CCDC6 was first discovered

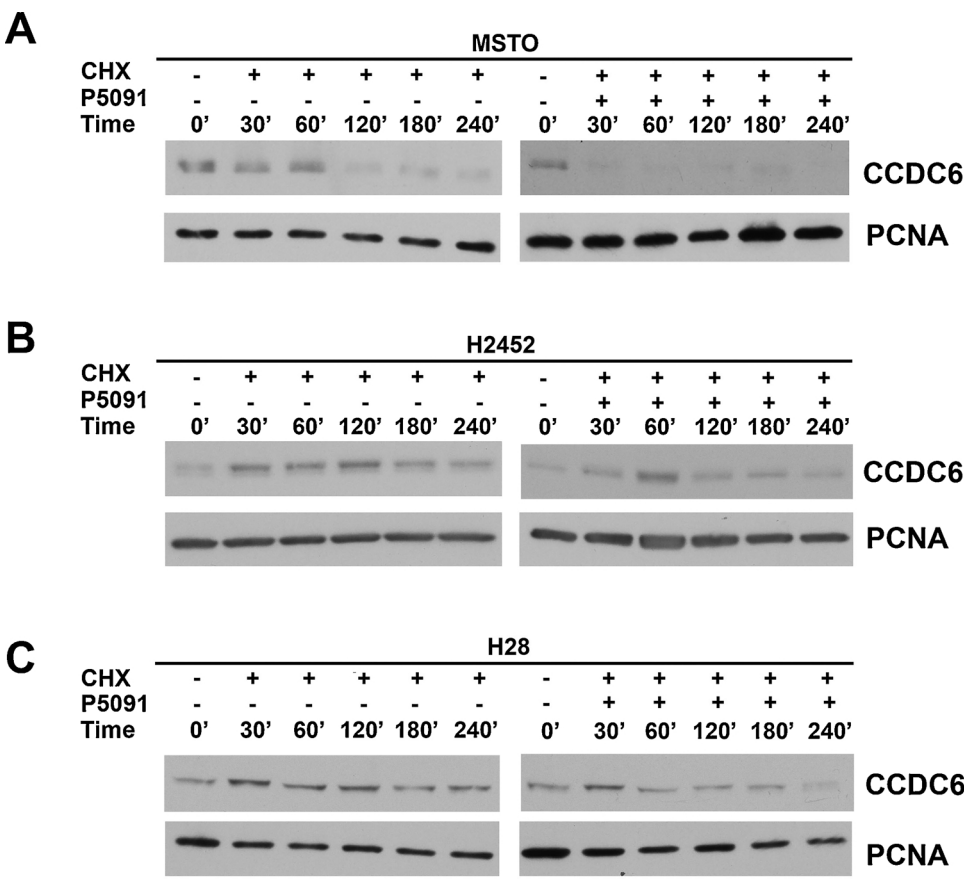

Fig. 2. P5091 affects CCDC6 half-life in MPM cells. MSTO-211H (A), H2452 (B) and H28 (C) cells were pre-treated with either vehicle or P5091 (12.5 μM) for 4 h, followed by the addition of cycloheximide (CHX) at 50 μg/ml for the indicated times. Total proteins lysates were subjected to immunoblot analysis using anti-CCDC6 or anti-PCNA antibodies as loading control.

because rearranged with the tyrosine kinase RET in papillary thyroid cancers [30]. Then, it has been found rearranged with RET also in colorectal carcinomas and in non-small cell lung cancers (NSCLCs) [31,32]. In CCDC6/RET rearranged cells the first 101 aminoacids of CCDC6 fused to RET, exert a dominant negative effect over the wild-type CCDC6 codified by the non-rearranged allele [33]. Although the frequency of CCDC6/RET rearrangement in NSCLCs is quite low, CCDC6 is expressed at low levels in a significative percentage of NSCLCs (about 30%), conferring chemotherapy resistance and PARP-inhibitor sensitivity [34,35]. Remarkably, CCDC6 low levels indicate poor prognosis correlating positively with the presence of lymph node metastasis and negatively with the disease free survival [35]. It has been reported that CCDC6 by interacting with CREB1 controls its transcriptional activity in a SUMO2 dependent manner [36,37]. Recently, computational analyses have predicted the CCDC6 interaction with BAP1, the deubiquitinase of the BRCA1 complex [38]. Given that both proteins are involved in DNA repair mechanisms by HR, our aim in this study has been to investigate the role of CCDC6, in predicting the response to PARP-inhibitors in MPM cell systems also carrying BAP1 mutations. Moreover, we performed the analysis of CCDC6 protein expression with its de-ubiquitinase USP7 in a panel of 34 MPM primary samples, that were characterized for BAP1 defects.

2. Methods

2.1. Tumor samples, TMA and immunohistochemical (IHC) analysis

40 tumor samples, from male and female patients, smokers and non-smokers, exposed to asbestos or not, were obtained from the Pathology Section of the Cardarelli Hospital of Naples, with the informed consent and protection of privacy. After surgical resection, the tissues were fixed in 10% formalin and included in paraffin blocks. The sections (4 μm) were stained with hematoxylin and eosin (H&E), or processed for immunohistochemistry with anti- CCDC6, USP7 and BAP1 antibodies.

Tissue Micro-Array (TMA) was built using the most representative areas from each single case. Tissue cylinders with a diameter of 0.3 mm were punched from morphologically representative tissue areas of each and brought into one recipient paraffin block (3 × 2.5 cm) using a semiautomated tissue arrayer (Galileo TMA, Milan, Italy) [39].

The immunoassayed TMA glass slide was digitalized with an Aperio AT2 digital pathology slide scanner (Leica Biosystems Nussloch GmbH)

The immunostaining of CCDC6, USP7 and BAP1 was quantitatively evaluated by determining the H-score expressed as 4 tier score of staining intensity by percentage of positive cells. The H-score was calculated by QuPath image software analysis [40].

2.2. Statistical analysis

Statistical analysis was performed using SPSS software (IBM Corp. Released 2013. IBM SPSS Statistics for Windows, Version 22.0. Armonk, NY: IBM Corp.). In order to correlate the expression levels between the three tissue biomarkers (CCDC6, USP7 and BAP1) a Spearman correlation test was performed [41].

2.3. Cell lines, drugs and chemicals

Malignant pleural mesothelioma cell lines, MSTO-211H, NCI-H2452 and NCI-H28, were purchased from ATCC (American Type Culture Collection) and were maintained in RPMI (Gibco, Paisley, UK), supplemented with 10% fetal bovine serum (FBS; Gibco BRL, Italia), 1% L-Glutamine and 1% of penicillin – streptomycin (Gibco, Paisley, UK).

Olaparib (AZD2281) and P005091 were provided by SelleckChem. The cycloheximide and the cisplatinum were from SIGMA-Aldrich.

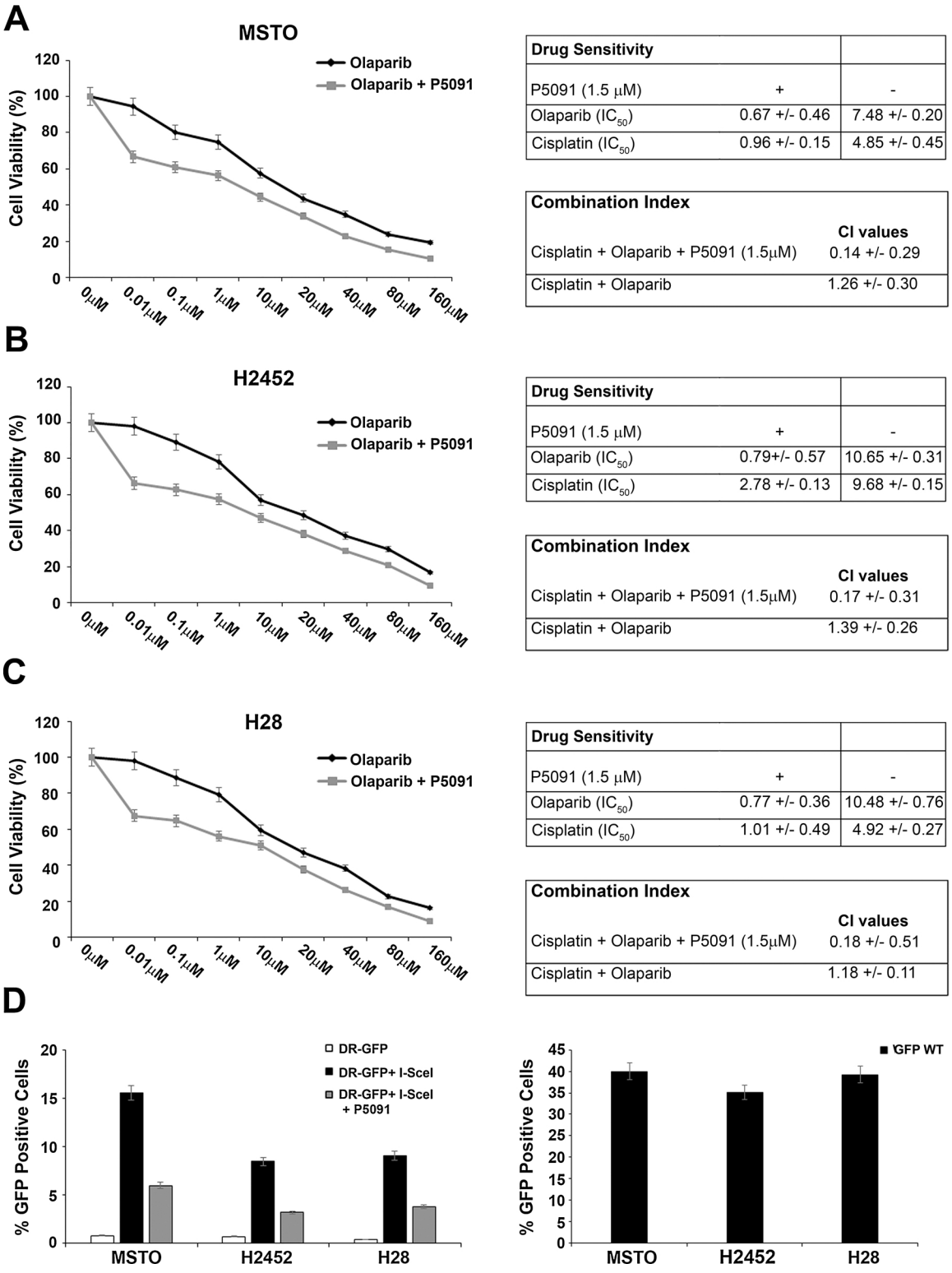

Drug Sensitivity		
P5091 (1.5 μM)	+	-
Olaparib (IC_{50})	0.67 +/- 0.46	7.48 +/- 0.20
Cisplatin (IC_{50})	0.96 +/- 0.15	4.85 +/- 0.45

Combination Index	
	CI values
Cisplatin + Olaparib + P5091 (1.5μM)	0.14 +/- 0.29
Cisplatin + Olaparib	1.26 +/- 0.30

Drug Sensitivity		
P5091 (1.5 μM)	+	-
Olaparib (IC_{50})	0.79+/- 0.57	10.65 +/- 0.31
Cisplatin (IC_{50})	2.78 +/- 0.13	9.68 +/- 0.15

Combination Index	
	CI values
Cisplatin + Olaparib + P5091 (1.5μM)	0.17 +/- 0.31
Cisplatin + Olaparib	1.39 +/- 0.26

Drug Sensitivity		
P5091 (1.5 μM)	+	-
Olaparib (IC_{50})	0.77 +/- 0.36	10.48 +/- 0.76
Cisplatin (IC_{50})	1.01 +/- 0.49	4.92 +/- 0.27

Combination Index	
	CI values
Cisplatin + Olaparib + P5091 (1.5μM)	0.18 +/- 0.51
Cisplatin + Olaparib	1.18 +/- 0.11

Fig. 3. CCDC6 downregulation affected the DSB repair by homologous recombination and enhanced the PARP-inhibitor sensitivity in BAP1 wt and mutant mesothelioma cells.

Left: Surviving fractions of MSTO-H211 (A), H2452 (B) and H28 (C) cells treated with olaparib at the indicated doses for 144 h. in presence or absence of P5091 (1.5 μM). Right: Drugs sensitivity to olaparib and cisplatin, in presence or absence of P5091 (1.5 μM), was determined in MSTO-H211, H2452 and H28 cells by a modified 3-(4,5-dimethylthiazole-2-yl)-2-5-diphenyltetrazolium bromide assay, CellTiter 96 Aqueous One Solution assay (Promega), as 50% inhibitory concentration (IC50) values. Combination index (CI) according to 1:2 concentration ratio of cisplatin and olaparib, in presence or absence of P5091 (1.5 μM), are shown. CI < 1, CI = 1, CI > 1 indicate synergism, additive effect and antagonism, respectively. The values are presented as mean standard deviation of three independent experiments. (D) MSTO-H211, H2452 and H28 cells were pretreated with either vehicle or P5091 ([3.92 μM IC50] in MSTO-H211 cells; [2.95 μM IC50] in H2452 cells; and [4.72 μM IC50] in H28 cells) for 4 h and transfected with DR-GFP alone, as control, or together with I-SceI. The percentages of GFP positive cells, compared to controls, were plotted as histograms, representative of the mean of three independent experiments. Error bars indicate the measurement of the standard error mean. The transfection efficiency has been plotted on the histograms shown on the right.

A

Drug Sensitivity		
Cell line	Olaparib P5091 1,5 μM	Olaparib
H2452^{EV}	0.71 +/- 0.27	10.14 +/- 0.30
H2452^{CCDC6+}	1.93 +/- 0.23	9.64 +/- 0.28

B

Drug Sensitivity		
Cell line	Olaparib P5091 1,5 μM	Olaparib
H28^{EV}	0.75 +/- 0.31	10.57 +/- 0.16
H28^{CCDC6+}	2.44 +/- 0.25	10.11 +/- 0.38

C

Drug Sensitivity		
Cell line	Olaparib P5091 1,5 μM	Olaparib
H2452^{EV}	0.71 +/- 0.27	10.14 +/- 0.30
H2452^{BAP1+}	0.90 +/- 0.38	15.72 +/- 0.23

D

Drug Sensitivity		
Cell line	Olaparib P5091 1,5 μM	Olaparib
H28^{EV}	0.75 +/- 0.31	10.57 +/- 0.16
H28^{BAP1+}	0.96 +/- 0.34	13.84 +/- 0.27

E

Drug Sensitivity	
Cell line	Olaparib (μmol/L)
MSTO ShCTRL	7.70 +/- 0.32
MSTO ShCCDC6	1.02 +/- 0.28
MSTO EV	7.69 +/- 0.35
MSTO BAP1 Δ	3.35 +/- 0.36
MSTO ShCCDC6 + BAP1 Δ	0.74 +/- 0.33

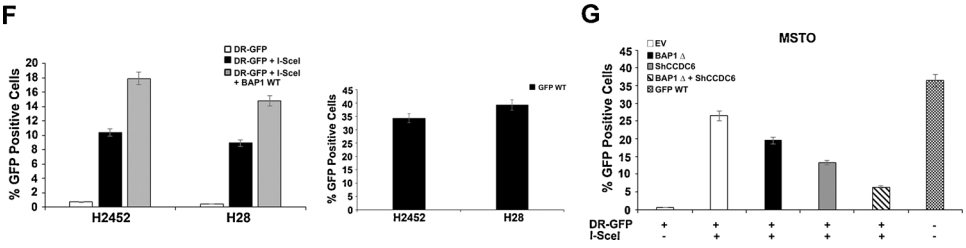

Fig. 4. CCDC6 overexpression, in presence of P5091, reduces the sensitivity to olaparib. In H2452 (A–C) and H28 (B–D) cells, transfected with CCDC6wt (H2452CCDC6 +, H28CCDC6 +), BAP1wt (H2452BAP1 +, H28BAP1 +) or the empty vector (H2452EV and H28EV), the drug sensitivity to olaparib, in presence or absence of P5091 [1.5 μM], was determined by a modified 3-(4,5-dimethylthiazole-2-yl)-2-5-diphenyltetrazolium bromide assay, CellTiter 96 Aqueous One Solution assay (Promega), as 50% inhibitory concentration (IC50) values. The values represent the mean +/- s.e.m. of three independent experiments. (E) CCDC6 silencing (shCCDC6) combined with a BAP1 deletion mutant (BAP1Δ221-238) expression determined olaparib sensitivity in BAP1wt MPM cells. The drugs sensitivity has been evaluated as in A–D. (F) BAP1wt overexpression enhances the HR-DNA repair proficiency in BAP1 mutant cells. H2452 and H28 cells were transfected as indicated for 48 h. The percentages of GFP positive cells were plotted as histograms representative of three independent experiments. Error bars indicate the standard error mean. The transfection efficacy has been plotted on the histograms shown on the right.
(G) The MSTO-211H cells were transiently transfected with BAP1Δ221-238, shCCDC6 or BAP1Δ221-238 plus shCCDC6 plasmids and the HR-reporter assay was performed. The percentages of GFP positive cells, compared to controls, were plotted as histograms representative of three independent experiments. Error bars indicate the standard error mean. The transfection efficiency has been plotted on the last bar of the graph upon GFP wild type (GFPwt) transfection.

2.4. Reagents and antibodies

For the biochemical analysis the antibodies anti – CCDC6 (ab56353) Abcam, the anti-tubulin (T6557) SIGMA-Aldrich, the anti-PCNA (NANO3) Millipore, the anti-BAP1 (sc-28383) and anti-Myc (9E10) sc-40 Santa Cruz Biotechonology (USA), were utilized. For the Immunoistochemical analysis the anti-CCDC6 (HPA – SIGMA) and the anti-USP7 (A300-033A – Bethyl) were utilized. The secondary antibodies were from Biorad, California.

2.5. Sensitivity test and design for drug combination

Antiproliferative activity was determined by the CellTiter 96 AQueous One Solution Cell Proliferation Assay (Promega), in terms of 50% inhibitory concentration (IC50) values.

The cells were plated in triplicate in 96-well plates at a density of 800 cells per well, and continuously exposed to each drug for 144 h. Each assay was performed in triplicate and IC50 values were expressed as mean +/- standard deviation.

The results of the combined treatment were analysed by using the CompuSyn software. The resulting combination index (CI) is a quantitative measure of the degree of interaction between different drugs. CI = 1 denotes additivity, CI > 1 denotes antagonism and CI < 1, it denotes synergism.

2.6. Protein extract and western blot analysis

Total cell extracts (TCE) were prepared with lysis buffer (50 mM Tris – HCl pH 7.5, 150 mM NaCl, 1% Triton X-100, 0.5% Sodium Deoxycholate, 0.1% SDS) and a mix of protease inhibitors. Protein concentration was estimated by a modified Bradford assay (Bio-Rad). For Western blotting, cell lysates were separated by SDS-PAGE (10% polyacrylamide) and the proteins were transferred to a PVDF membrane. Membranes were blocked with 5% TBS-BSA and incubated with the primary antibodies [42,43]. Immunoblotting experiments were carried out according to standard procedures and visualized using the ECL chemiluminescence system (Amersham/Pharmacia Biotech). As a control for equal loading of protein lysates, the blotted proteins were probed with antibody against anti-γ-tubulin protein.

2.7. Apoptosis assay

The MPM cell lines, MSTO-211H, NCI-H2452 and NCI-H28 were treated with 12.5 μM and 25 μM of P5091 for 24 h. Apoptosis was quantified by measuring Caspase 3/7 activation using the Caspase-Glo 3/7 assay (Promega) according to the manufacturer's instructions.

2.8. Plasmids and transfection

PcDNA4ToA-CCDC6 and BAP1 WT plasmids were transfected in NCI-H2452 and NCI-H28 cells with FuGene HD (Promega). CCDC6 shRNA (pLKO.1 puro) was from Sigma-Aldrich. MSTO-211H cells were transfected with BAP1Δ or with a plasmid pool (shCCDC6, NM_005436) for transient CCDC6 silencing by Fugene (Promega) for 48 h. The DR-GFP reporter plasmid is based on a construct developed by M. Jasin [44] and contains two mutated GFP genes.

2.9. HR assay

MPM cells were plated in a 60 mm plate and transfected with the DR-GFP reporter alone (as negative control), or together with the I-SceI gene. Wild type GFP was used as control for transfection efficiency. After 48 h cells were collected and analyzed by FACS analysis with BD Accuri C6 Flow Cytometer (BD Bioscience, Canada).

3. Results

3.1. CCDC6 protein levels in mesothelioma cell lines are modulated by the USP7 inhibitor P5091

P5091 is a specific inhibitor of the deubiquitinase USP7. The compound was shown to impair the protein stability of HDM2 induced by USP7 which resulted in the stabilization of p21 and p53. However, p53 negative cells were also sensitive to P5091, suggesting a p53-independent mechanism [45]. Recent investigations on USP7 inhibitor have shown antitumor properties also in vivo in several tumors types

Table 1
Detailed distribution of H-scores along with 50th percentile and quartiles samples stratification (SEX: F = FEMALE / M = MALE; SMOKE: Y = YES / N = NO; ASBESTOS: Y = YES / N = NO; LOCALIZATION: N = NUCLEUS / C = CYTOPLASM; HISTOLOGIC TYPE: E = EPITHELIOID / M = MIXED / S = SARCOMATOID).

	CCDC6			USP7			BAP1								
N.	**H-score**	**50th percentile**	**Quartiles**	**H-score**	**50th percentile**	**Quartiles**	**H-score**	**50th percentile**	**Quartiles**	**SEX**	**SMOKE**	**ASBESTOS**	**BAP1 LOC**	**CCDC6 LOC**	**HISTOL. TYPE**
1	164,75	HIGH	4	24,31	HIGH	3	6,86	LOW	2	F	Y	N		C	E
2	105,93	LOW	2	17,77	LOW	2	5,99	LOW	2	F	Y	N		NC	E
3	113,83	HIGH	3	65,34	HIGH	4	96,74	HIGH	4	F	Y	N			E
4	124,74	HIGH	3	34,94	HIGH	3	11,88	LOW	2	F	Y	N		C	M
5	61,53	LOW	1	14,32	LOW	2	54,41	HIGH	4	F	N	N	C	C	E
6	30,58	LOW	1	9,56	LOW	1	9,13	LOW	2	F	N	N		C	E
7	126,76	HIGH	3	89,29	HIGH	4	8,91	LOW	2	F	N	N	C	C	E
8	136,20	HIGH	3	16,07	LOW	2	51,75	HIGH	3	F	N	N		C	E
9	71,92	LOW	1	16,94	LOW	2	3,61	LOW	2	F	NA	NA		C	E
10	91,64	LOW	2	48,61	HIGH	3	0,85	LOW	1	M	Y	Y		C	M
11	208,31	HIGH	4	115,55	HIGH	4	82,78	HIGH	4	M	Y	Y		NC	E
12	96,69	LOW	2	56,08	HIGH	4	56,10	HIGH	4	M	Y	Y			E
13	101,22	LOW	2	66,44	HIGH	4	13,86	LOW	2	M	Y	Y		C	E
14	159,22	HIGH	4	28,81	HIGH	3	119,47	HIGH	4	M	Y	N		NC	E
15	112,51	LOW	2	17,97	LOW	2	0,11	LOW	1	M	Y	N		C	E
16	141,63	HIGH	3	4,80	LOW	1	38,67	HIGH	3	M	Y	N		C	E
17	84,05	LOW	1	18,21	HIGH	3	3,30	LOW	2	M	Y	N		C	E
18	106,72	LOW	2	16,03	LOW	2	15,04	HIGH	3	M	Y	N			E
19	111,46	LOW	2	21,82	HIGH	3	0,50	LOW	1	M	Y	N		NC	E
20	202,73	HIGH	4	65,90	HIGH	4	17,27	HIGH	3	M	Y	N		NC	E
21	193,04	HIGH	4	21,25	HIGH	3	66,78	HIGH	4	M	Y	N		NC	E
22	205,27	HIGH	4	65,09	HIGH	4	3,19	LOW	1	M	Y	N		C	E
23	168,66	HIGH	4	0,44	LOW	1	5,13	LOW	2	M	N	Y		C	E
24	160,29	HIGH	4	48,37	HIGH	3	101,88	HIGH	4	M	N	N		NC	E
25	117,24	HIGH	3	14,91	LOW	2	0,33	LOW	1	M	N	N		C	E
26	77,03	LOW	1	10,64	LOW	2	2,26	LOW	1	M	N	N		C	E
27	137,12	HIGH	3	63,14	HIGH	4	52,65	HIGH	3	M	NA	NA		C	E
28	47,74	LOW	1	2,89	LOW	1	35,74	HIGH	3	M	NA	NA		C	S
29	149,25	HIGH	3	8,23	LOW	1	35,04	HIGH	3	M	NA	NA			S
30	134,50	HIGH	3	33,78	HIGH	3	147,51	HIGH	4	M	NA	NA		C	E
31	76,40	LOW	1	15,20	LOW	2	19,10	HIGH	3	M	NA	NA		C	E
32	38,35	LOW	1	0,00	LOW	1	35,87	HIGH	3	M	NA	NA	N + C	C	E
33	102,85	LOW	2	2,28	LOW	1	0,55	LOW	1	M	NA	NA		NC	E
34	87,33	LOW	2	4,03	LOW	1	1,11	LOW	1	M	NA	NA		C	E

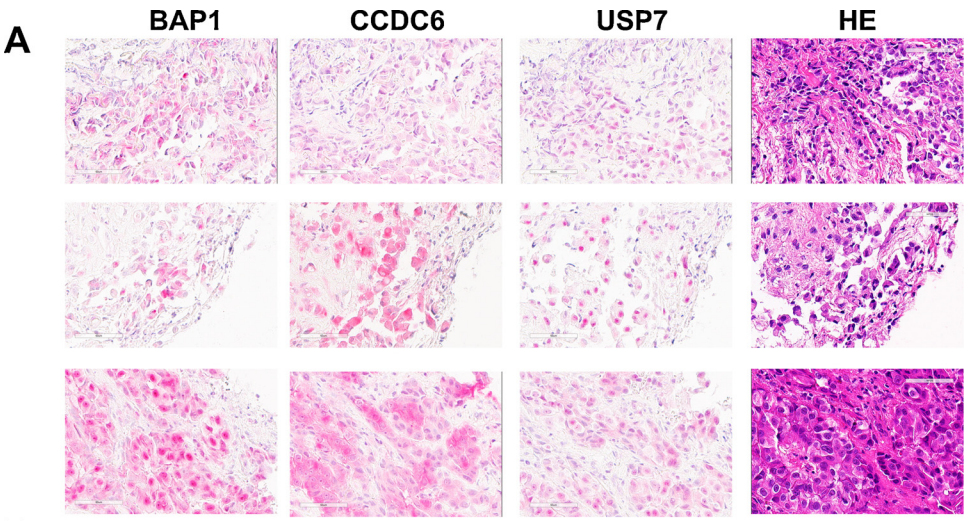

Fig. 5. Immunohistochemistry analysis of a MPM TMA. (A) The panel shows three representative images of different Malignant Pleural Mesothelioma samples immunostained for BAP1, CCDC6 and USP7 proteins that exhibits different intensity of expression. The staining for hematoxylin/eosin is shown on the right (magnification 40 x). (B) The 2-tailed Spearman Rank correlation test between CCDC6 and USP/ H-score values proved to be extremely significant across all the tumor samples.

B

Correlations

			CCDC6num	USP7num	BAPnum
Spearman's rho	CCDC6	Correlation Coefficient	1,000	,448**	,267
		Sig. (2-tailed)		,008	,127
		N	34	34	34
	USP7	Correlation Coefficient	,448**	1,000	,257
		Sig. (2-tailed)	,008		,275
		N	34	34	34
	BAP	Correlation Coefficient	0,267	0,257	1,000
		Sig. (2-tailed)	0,127	0,143	
		N	34	34	34

**. Correlation is significant at the 0.01 level (2-tailed)

[46]. Interestingly, the inhibition of USP7 can alter the turnover of CCDC6 prompting its use in combination with PARP inhibitors in new therapeutic approaches for lung, prostate and bladder cancer [35,47–49]. In this work we analyzed the cytostatic effect induced by USP7 inhibition P5091 on the pleural tumor cell growth. MSTO-211H, H2452 and H28 mesothelioma cell lines, that showed appreciable levels of CCDC6 and USP7 (Fig. 1A), were treated with vehicle or various concentrations of P5091 for 144 h: P5091 treatment decreased the viability of mesothelioma cells (Fig. 1B–D), by inducing an increase in apoptotic cells number, as shown by the activation of the caspase 3 (Fig. 1E).

Next, we asked whether the USP7 inhibitor, P5091, affected the stability of CCDC6 protein in the mesothelioma cell lines. Thus, MSTO-211H, H2452 and H28 cells, that expressed appreciable levels of CCDC6 and USP7 proteins were pre-treated with either vehicle or P5091 for 4 h, followed by the addition of cycloheximide (50 μg/ml), to block new protein synthesis, for the indicated times. The immunoblot with anti-CCDC6 antibody indicated that the CCDC6 half-life was reduced upon the P5091 pretreatment in all the cell lines. Thus, P5091 accelerated the degradation of CCDC6 versus control cycloheximide-alone treated MSTO-211H, H2452 and H28 mesothelioma cells (Fig. 2A–C).

3.2. CCDC6 downregulation enhances the PARP-inhibitor sensitivity in BAP1 wt and mutant mesothelioma cells

Nearly 50% of MPM carry somatic inactivating mutations in the tumor suppressor BAP1 gene, with consequent defects in the HR DNA repair pathway [23]. However, in the search for novel treatments, the PARP inhibitors niraparib and olaparib have been tested in vitro and reported to be significantly cytotoxic in a series of MPM cell lines, regardless of the BAP1 protein status (wt or mutant) [50]. These observations suggested that, besides BAP1 mutations, other molecular alterations affecting HR DNA repair, might be responsible of PARP1 sensitivity in MPM.

In our work, we have treated MPM cell lines, carrying BAP1 in a wild type or mutant form [the MSTO-211H (BAP1 wt), the H2452 (BAP1A95D) and the H28 (BAP1 intron6/exon7 deleted)], with the PARP-inhibitor olaparib and observed that the growth inhibition was disrespectful of the BAP1 mutational status. Since the MPM cell lines expressed an amount of CCDC6 protein targetable with P5091 treatment, we tested the sensitivity of these cells to the PARP-inhibitor olaparib in presence of P5091. The sensitivity of mesothelioma cell lines to the PARP-inhibitor olaparib was enhanced by the CCDC6 downregulation induced by the USP7 inhibitor P5091 [MSTO-H211: IC50 ≥ 7 μM vs 0.67 μM, in presence of 1.5 μM P5091; H2452: IC50 ≥ 10 μM vs 0.79 μM, in presence of 1.5 μM P5091; H28: IC50 ≥ 10 μM vs 0.77 μM in presence of 1.5 μM P5091] (Fig. 3A–C).

Next, in order to understand to what extent the sensitivity of MPM cells to PARP-inhibitors was dependent on the BAP1 mutations or on the CCDC6 levels (modulated by P5091), we overexpressed the CCDC6wt or the BAP1wt both in the BAP1 mutant MPM cells, treated or not with P5091. In the BAP1 mutant H2452 and H28 cells treated with the USP7 inhibitor P5091, the CCDC6 re-expression, reduced the sensitivity to olaparib (Fig. 4A, B; Supplementary Fig. 1), while the BAP1 wt overexpression determined a mostly unmodified sensitivity to olaparib in comparison to untransfected cells (Fig. 4C, D; Supplementary Fig. 1). Furthermore, the silencing of CCDC6 in the BAP1 wt MSTO-211H cells, caused an increased sensitivity to the PARP-inhibitor olaparib, in a comparable manner to what observed upon USP7 inhibition (Fig. 4E). Interestingly, in the same cells the overexpression of a BAP1 mutant, BAP1Δ221-238, enhanced olaparib sensitivity (Fig. 4E; Supplementary Fig. 1).

3.3. CCDC6 downregulation affects the DSB repair by homologous recombination in BAP1 wt and mutant mesothelioma cells

The BAP1Δ221-238 mutation has been recently identified in mesothelioma primary cells and in vitro characterized as capable to impair the HR-DNA repair [24]. Then, we investigated the ability to repair the DNA double strand breaks by homologous recombination in the MPM cells by modulating CCDC6 levels or blocking BAP1 activity.

After transfection of the reporter DR-GFP plasmid and the breaking enzyme I-SceI gene, able to induce DSBs, we compared the efficacy of the DNA repair by HR in all the cells, in presence or absence of P5091, lowering CCDC6 levels. The H2452 and the H28 BAP1 mutant cells exhibited a lower proficiency in DNA repair by HR, compared to the BAP1 wt MSTO-211H cells (Fig. 3D). However, the BAP1 wt vector overexpression restored the HR proficiency in the BAP1 mutant cells, as detected by GFP reporter assay (Fig. 4F), while the transfection of the BAP1Δ221-238 was capable to impair the HR DNA repair in the MSTO-211H mesothelioma cells (Fig. 4G; Supplementary Fig. 2). Most importantly, the combination of both CCDC6 silencing and BAP1Δ221-238 overexpression amplified the effects on the DNA repair process and enhanced the effect of PARP-inhibitor as reported in the previous paragraph (Fig. 4E, G).

Interestingly, by immunoprecipitation assay, we proved that endogenous CCDC6 interacted specifically, as predicted, with BAP1 [38]. The truncated isoform of CCDC6 (1-223) still coimmunoprecipitated with BAP1, suggesting that the aminoterminus of CCDC6 is sufficient for the CCDC6 binding to BAP1. In mesothelioma cells, CCDC6 and BAP1 showed biochemical interaction that could explain the interplay between the two proteins, that needs further characterization (Supplementary Fig. 3).

3.4. Immunohistochemical evaluation of expression levels of CCDC6 and of the deubiquitinase USP7, in a collection of primary mesothelioma tumors organized in a "tissue micro array"

For the purpose of assessing CCDC6 expression levels in a group of human MPM tumors, we analyzed 40 samples from patients who underwent diagnostic surgical tumor biopsies without neo adjuvant treatments. The patient characteristics are listed in Table 1. The immunostaining showed that the CCDC6 expression levels mostly correlated with the protein levels of its deubiquitinating enzyme, USP7 (Table 1 and Fig. 5A). Out of 40 analyzed cores, we could assess the expression of both proteins, CCDC6 and USP7, only in 34 samples.

More precisely, TMA (Tissue Micro Array) immunostaining for CCDC6 expression demonstrated that the protein was barely detectable (low range H-scores) in about 24% of the analyzed samples (8/34). This result is in accordance with the data reported in lung tumors [34,47].

We also analyzed the expression of USP7 protein in the 34 samples. A whole list of CCDC6 and USP7 score of intensity with the relative frequencies in the 40 examined TMA cores, including the missing samples, is resumed in Table 1. Notably, in about 70% of the samples (24/34) the expression levels of CCDC6 and USP7 matched. Of notice, the H index of both the proteins was high in almost 50% of the samples.

Rank correlation analysis based on 2-tailed non-parametric Spearman test resulted of statistical significance ($p = 0.001$), being the correlation considered significant at $p = 0.01$ (Fig. 5B).

Finally, we evaluated the BAP1 expression in the same set of samples (Fig. 5A). The immunostaining of the TMA revealed that BAP1 deubiquitinase was absent or localized in the cytosol in 50% of the samples (17/34). BAP1 expression was barely detectable (1 st quartile of H-score distribution) in 8 samples, while BAP1 was detected in the nucleus in the remaining samples, and fell into the 2nd or 3rd quartile (Table 1). The BAP1 depletion or the BAP1 exclusion from the nucleus are associated to a BAP1 mutational status and its loss of function, while a nuclear BAP1 depicts a wild type protein, and a conserved function [51]. The analysis of our data based on immunohistochemical stainings indicated that nearly 30% of the MPM biopsies exhibited impaired BAP1 and low levels of CCDC6.

4. Discussion

MPM prognosis is still very poor despite huge efforts in identifying new drug targetable genetic alterations [11]. So far, the therapeutic actions for mesothelioma are limited by the late stage of diagnosis and the intrinsic chemo-resistance of the tumor. The standard therapy for MPM is based on cisplatin and pemetrexed with a mean overall survival of about 12 months and a median progression free survival of less than 6 months. Thus, novel therapeutic approaches are urgently needed. In recent years, for lung cancer and breast cancer, druggable oncogenic alterations have been identified and targeted therapy has represented an important option for treatment in solid tumors. For MPM, to date, no oncogene driver mutation that may be responsive to targeted therapies has been identified and clinical guidelines do not recommend biological targeted therapy, even if a variety of biological agents have been tested both at pre-clinical and clinical level against over-expressed targets or deregulated signaling pathways, with uncertain results.

BAP1 has been reported as the most mutated gene in MPM, regardless of ethnic background or other clinic characteristic. BAP1 has been postulated to have a role in HR DNA repair and in cell cycle and requires a nuclear localization for its identified activities. Somatic BAP1 mutations are reported in sporadic MPM in about 50% of analyzed biopsies at IHC level. Currently, BAP1 is used to discriminate, in cases of doubt, between inflammatory and neoplastic lesions [https://www.aiom.it/linee-guida/linee-guida-aiom-2018-mesotelioma-pleurico/].

In the context of cancers with compromised HR repair, the inhibition of PARP causes a collapse in the base excision repair pathway and results in the accumulation of single strand breaks that end up in DSBs upon DNA replication [52–55]. The olaparib efficacy in killing the MPM cells has been proved in preclinical studies [24;50]. However, BAP1 alterations do not predict the response of MPM patients to a target therapy that includes the PARP inhibition treatment.

Here we reported that about 30% of the MPMs express low levels of the CCDC6, a protein involved in HR DNA repair. We have verified that olaparib is efficient in killing MPM cells expressing low levels of CCDC6. A first mesothelioma Phase II clinical trial involving olaparib (NCT03531840), “based on somatic or germline mutation status of DNA repair genes” has been launched on July 2018 and results are expected by December 2020.

For the MPMs expressing appreciable amount of CCDC6 protein we have provided evidences in order to propose a different therapeutic approach. CCDC6 protein levels are finely regulated by the E3 ubiquitin ligase Fbxw7, which addresses CCDC6 to proteasome degradation, and by the deubiquitinase USP7 that stabilizes it. We have demonstrated that in the NSCLC cells that express normal levels of CCDC6, the USP7 inhibitor, P5091, sensitize lung cancer cells to olaparib by lowering CCDC6 levels [35]. Remarkably, we have described the same also in cells derived from neuroendocrine small cell lung cancers (SCLCs), in hormone-sensitive and castration-resistant prostate cancer cells, and recently in bladder cancer cells [47–49]. Thus, we have proved that MPM cells expressing normal level of CCDC6 can be sensitized to olaparib by P5091.

CCDC6 has been predicted to interact with BAP1 [38]. Indeed, we verified that endogenous CCDC6 interacts specifically with BAP1 in 293 T cells. The myc-tagged CCDC6 truncated mutant (1-223) still coimmunoprecipitated with BAP1, suggesting that the aminoterminus of CCDC6 is sufficient for the binding to BAP1 (Supplementary Fig. 3). Moreover, we confirmed the CCDC6 interaction with BAP1 in the mesothelioma model of MSTO-221H cells, carrying BAP1 wild type and in the H2452 cells carrying the BAP1A95D mutant (Supplementary Fig. 3). In the MSTO-211H cells, the overexpression of a BAP1 mutant (BAP1Δ221-238) determined an impairment of the HR-DNA repair, and increased the sensitivity to the PARP-inhibitor olaparib. Nevertheless,

the silencing of CCDC6 in the same cells caused an impairment of HR and enhanced the olaparib sensitivity. Noteworthy, the combination of both the CCDC6 silencing with the BAP1 mutant (BAP1Δ221-238) overexpression amplified the effects inducing a stronger impairment of the HR-DNA repair and enhancing cancer cell sensitivity to the PARP-inhibitor sensitivity (Fig. 4F, G).

The TMA analysis confirmed the expected frequency of BAP1 mutant samples according to recent reports [51]. Moreover, 30% of the MPM biopsies that exhibited absent or low staining for CCDC6 were also carrying BAP1 mutations.

Then, our data suggest that the two proteins might cooperate in response to DNA damage in coordinating the DNA repair by HR. In the clinic, BAP1 alterations might be required but not sufficient to induce PARP inhibitors sensitivity. We can hypothesize that upon ATM activation which phosphorylates CCDC6 at threonine 434 and BAP1 at serine 592, the cross-talk between the two proteins might culminate in the activation of BRCA1 to coordinate the DNA repair by HR.

We believe that the routinely IHC evaluation of CCDC6 and USP7 together with BAP1 could offer novel therapeutic options for personalized treatment to MPM patients.

In conclusion, we propose CCDC6 as a biomarker of drugs sensitivity for MPMs. In case of MPMs expressing low levels of CCDC6 the addition of olaparib to cisplatinum and pemetrexed is expected to be highly beneficial. In case of MPMs expressing normal CCDC6 levels the sensitivity to olaparib can be restored by the addition of P5091.

Aknowledgements

Our research has been supported by AIRC n 4592 to AC; POR Campania FSE 2007/2013 “CREME Campania Research for Experimental Medicine”, CNR-IEOS UOS Napoli; Ministero dell’Istruzione, dell’Università e della Ricerca” (MIUR), PRIN 2009T5NKTB_002 to AC; POR Campania FESR 2014-2020 “SATIN” grant.

We are grateful to Prof. Mario De Felice for his continuous support and encouragements. We are indebted to Rosaria Catalano for technical help.

Appendix A. Supplementary data

Supplementary material related to this article can be found, in the online version, at doi:https://doi.org/10.1016/j.lungcan.2019.07.011.

References

[1] T.A. Yap, J.G. Aerts, S. Popat, D.A. Fennell, Novel insights into mesothelioma biology and implications for therapy, Nat. Rev. Cancer 17 (475) (2017) 88.
[2] J.C. Wagner, C.A. Sleggs, P. Marchand, Diffuse pleural mesothelioma and asbestos exposure in the North Western Cape Province, Br. J. Ind. Med. 17 (1960) 260–271.
[3] M. Carbone, H. Yang, Mesothelioma: recent highlights, Ann. Transl. Med. 5 (2017) 238.
[4] C. Bianchi, L. Giarelli, G. Grandi, A. Brollo, L. Ramani, C. Zuch, Latency periods in asbestos-related mesothelioma of the pleura, Eur. J. Cancer Prev. 6 (1997) 162–166.
[5] M. Carbone, S. Kanodia, A. Chao, A. Miller, A. Wali, D. Weissman, A. Adjei, F. Baumann, P. Boffetta, B. Buck, M. de Perrot, A.U. Dogan, S. Gavett, A. Gualtieri, R. Hassan, M. Hesdorffer, F.R. Hirsch, D. Larson, W. Mao, S. Masten, H.I. Pass, J. Peto, E. Pira, I. Steele, A. Tsao, G.A. Woodard, H. Yang, S. Malik, Consensus report of the 2015 Weinman international conference on mesothelioma, J. Thorac. Oncol. 11 (2016) 1246–1262.
[6] H. Yang, Z. Rivera, S. Jube, M. Nasu, P. Bertino, C. Goparaju, G. Franzoso, M.T. Lotze, T. Krausz, H.I. Pass, M.E. Bianchi, M. Carbone, Programmed necrosis induced by asbestos in human mesothelial cells causes high-mobility group box 1 protein release and resultant inflammation, Proc. Natl. Acad. Sci. U. S. A. 107 (2010) 12611–12616.
[7] F. Qi, G. Okimoto, S. Jube, A. Napolitano, H.I. Pass, R. Laczko, R.M. Demay, G. Khan, M. Tiirikainen, C. Rinaudo, A. Croce, H. Yang, G. Gaudino, M. Carbone, Continuous exposure to chrysotile asbestos can cause transformation of human mesothelial cells via HMGB1 and TNF-α signaling, Am. J. Pathol. 183 (2013) 1654–1666.
[8] B.T. Mossman, A. Shukla, N.H. Heintz, C.F. Verschraegen, A. Thomas, R. Hassan, New insights into understanding the mechanisms, pathogenesis, and management of malignant mesotheliomas, Am. J. Pathol. 182 (2013) 1065–1077.
[9] N.J. Vogelzang, J.J. Rusthoven, J. Symanowski, C. Denham, E. Kaukel, P. Ruffie, U. Gatzemeier, M. Boyer, S. Emri, C. Manegold, C. Niyikiza, P. Paoletti, Phase III study of pemetrexed in combination with cisplatin versus cisplatin alone in patients with malignant pleural mesothelioma, J. Clin. Oncol. 21 (2003) 2636–2644.
[10] P.E. Van Schil, P. Baas, R. Gaafar, A.P. Maat, M. Van de Pol, B. Hasan, H.M. Klomp, A.M. Abdelrahman, J. Welch, J.P. van Meerbeeck, European Organisation for Research and Treatment of Cancer (EORTC) Lung Cancer group. Trimodality therapy for malignant pleural mesothelioma: results from an EORTC phase II multicentre trial, Eur. Respir. J. 36 (2010) 1362–1369.
[11] M.R. Mancuso, J.W. Neal, Novel systemic therapy against malignant pleural mesothelioma, Transl. Lung Cancer Res. 6 (2017) 295–314.
[12] G. Zalcman, J. Mazieres, J. Margery, L. Greillier, C. Audigier-Valette, D. Moro-Sibilot, O. Molinier, R. Corre, I. Monnet, V. Gounant, F. Rivière, H. Janicot, R. Gervais, C. Locher, B. Milleron, Q. Tran, M.P. Lebitasy, F. Morin, C. Creveuil, J.J. Parienti, A. Scherpereel, French Cooperative Thoracic Intergroup (IFCT). Bevacizumab for newly diagnosed pleural mesothelioma in the Mesothelioma Avastin Cisplatin Pemetrexed Study (MAPS): a randomised, controlled, open-label, phase 3 trial, Lancet 387 (2016) 1405–1414.
[13] R. Bueno, E.W. Stawiski, L.D. Goldstein, S. Durinck, A. De Rienzo, Z. Modrusan, F. Gnad, T.T. Nguyen, B.S. Jaiswal, L.R. Chirieac, D. Sciaranghella, N. Dao, C.E. Gustafson, K.J. Munir, J.A. Hackney, A. Chaudhuri, R. Gupta, J. Guillory, K. Toy, C. Ha, Y.J. Chen, J. Stinson, S. Chaudhuri, N. Zhang, T.D. Wu, D.J. Sugarbaker, F.J. de Sauvage, W.G. Richards, S. Seshagiri, Comprehensive genomic analysis of malignant pleural mesothelioma identifies recurrent mutations, gene fusions and splicing alterations, Nat. Genet. 48 (2016) 407–416.
[14] S. Kato, B.N. Tomson, T.P. Buys, S.K. Elkin, J.L. Carter, R. Kurzrock, Genomic landscape of malignant mesotheliomas, Mol. Cancer Ther. 15 (2016) 2498–2507.
[15] G. Guo, J. Chmielecki, C. Goparaju, A. Heguy, I. Dolgalev, M. Carbone, S. Seepo, M. Meyerson, H.I. Pass, Whole-exome sequencing reveals frequent genetic alterations in BAP1, NF2, CDKN2A, and CUL1 in malignant pleural mesothelioma, Cancer Res. 75 (2015) 264–269.
[16] M. Lo Iacono, V. Monica, L. Righi, F. Grosso, R. Libener, S. Vatrano, P. Bironzo, S. Novello, L. Musmeci, M. Volante, M. Papotti, G.V. Scagliotti, Targeted next-generation sequencing of cancer genes in advanced stage malignant pleural mesothelioma: a retrospective study, J. Thorac. Oncol. 10 (2015) 492–499.
[17] J.R. Testa, M. Cheung, J. Pei, J.E. Below, Y. Tan, E. Sementino, N.J. Cox, A.U. Dogan, H.I. Pass, S. Trusa, M. Hesdorffer, M. Nasu, A. Powers, Z. Rivera, S. Comertpay, M. Tanji, G. Gaudino, H. Yang, M. Carbone, Germline BAP1 mutations predispose to malignant mesothelioma, Nat. Genet. 43 (2011) 1022–1025.
[18] K. Rai, R. Pilarski, C.M. Cebulla, M.H. Abdel-Rahman, Comprehensive review of BAP1 tumor predisposition syndrome with report of two new cases, Clin. Genet. 89 (2016) 285–294.
[19] Y. Yoshikawa, M. Emi, T. Hashimoto-Tamaoki, M. Ohmuraya, A. Sato, T. Tsujimura, S. Hasegawa, T. Nakano, M. Nasu, S. Pastorino, A. Szymiczek, A. Bononi, M. Tanji, I. Pagano, G. Gaudino, A. Napolitano, C. Goparaju, H.I. Pass, H. Yang, M. Carbone, High-density array-CGH with targeted NGS unmask multiple noncontiguous minute deletions on chromosome 3p21 in mesothelioma, Proc. Natl. Acad. Sci. U.S.A. 113 (2016) 13432–13437.
[20] D.E. Jensen, M. Proctor, S.T. Marquis, H.P. Gardner, S.I. Ha, L.A. Chodosh, A.M. Ishov, N. Tommerup, H. Vissing, Y. Sekido, J. Minna, A. Borodovsky, D.C. Schultz, K.D. Wilkinson, G.G. Maul, N. Barlev, S.L. Berger, G.C. Prendergast, F.J. Rauscher 3rd, BAP1: a novel ubiquitin hydrolase which binds to the BRCA1 RING finger and enhances BRCA1-mediated cell growth suppression, Oncogene. 16 (1998) 1097–1112.
[21] H. Yu, H. Pak, I. Hammond-Martel, M. Ghram, A. Rodrigue, S. Daou, H. Barbour, L. Corbeil, J. Hébert, E. Drobetsky, J.Y. Masson, J.M. Di Noia, B. Affar el, Tumor suppressor and deubiquitinase BAP1 promotes DNA double-strand break repair, Proc. Natl. Acad. Sci. U.S.A. 111 (2014) 285–290.
[22] S. Peña-Llopis, S. Vega-Rubín-de-Celis, A. Liao, N. Leng, A. Pavía-Jiménez, S. Wang, T. Yamasaki, L. Zhrebker, S. Sivanand, P. Spence, L. Kinch, T. Hambuch, S. Jain, Y. Lotan, V. Margulis, A.I. Sagalowsky, P.B. Summerour, W. Kabbani, S.W. Wong, N. Grishin, M. Laurent, X.J. Xie, C.D. Haudenschild, M.T. Ross, D.R. Bentley, P. Kapur, J. Brugarolas, BAP1 loss defines a new class of renal cell carcinoma, Nat. Genet. 44 (2012) 751–759.
[23] I.H. Ismail, R. Davidson, J.P. Gagné, Z.Z. Xu, G.G. Poirier, M.J. Hendzel, Germline mutations in BAP1 impair its function in DNA double-strand break repair, Cancer Res. 74 (2014) 4282–4294.
[24] R. Parrotta, A. Okonska, M. Ronner, W. Weder, R. Stahel, L. Penengo, E. Felley-Bosco, A novel BRCA1-associated protein-1 isoform affects response of mesothelioma cells to drugs impairing BRCA1-mediated DNA repair, J. Thorac. Oncol. 12 (2017) 1309–1319.
[25] D. Branzei, M. Foiani, Regulation of DNA repair throughout the cell cycle, Nat. Rev. Mol. Cell Biol. 9 (2008) 297–308.
[26] F. Merolla, F. Pentimalli, R. Pacelli, G. Vecchio, A. Fusco, M. Grieco, A. Celetti, Involvement of H4(D10S170) protein in ATM-dependent response to DNA damage, Oncogene 26 (2007) 6167–6175.
[27] V. Turinetto, C. Giachino, Multiple facets of histone variant H2AX: a DNA double-strand-break marker with several biological functions, Nucleic Acids Res. 43 (2015) 2489–2498.
[28] F. Merolla, C. Luise, M.T. Muller, R. Pacelli, A. Fusco, A. Celetti, Loss of CCDC6, the first identified RET partner gene, affects pH2AX S139 levels and accelerates mitotic entry upon DNA damage, PLoS One 7 (2012) e36177.
[29] A. Cerrato, F. Merolla, F. Morra, A. Celetti, CCDC6: the identity of a protein known to be partner in fusion, Int. J. Cancer 142 (2018) 1300–1308.
[30] M. Grieco, M. Santoro, M.T. Berlingieri, R.M. Melillo, R. Donghi, I. Bongarzone,

M.A. Pierotti, G. Della Porta, A. Fusco, G. Vecchio, PTC is a novel rearranged form of the ret proto-oncogene and is frequently detected in vivo in human thyroid papillary carcinomas, Cell 60 (1990) 557–563.
[31] A.F. Le Rolle, S.J. Klempner, C.R. Garrett, T. Seery, E.M. Sanford, S. Balasubramanian, J.S. Ross, P.J. Stephens, V.A. Miller, S.M. Ali, V.K. Chiu, Identification and characterization of RET fusions in advanced colorectal cancer, Oncotarget 6 (2015) 28929–28937.
[32] K. Takeuchi, M. Soda, Y. Togashi, R. Suzuki, S. Sakata, S. Hatano, R. Asaka, W. Hamanaka, H. Ninomiya, H. Uehara, Y. Lim Choi, Y. Satoh, S. Okumura, K. Nakagawa, H. Mano, Y. Ishikawa, RET, ROS1 and ALK fusions in lung cancer, Nat. Med. 18 (2012) 378–381.
[33] A. Celetti, A. Cerrato, F. Merolla, D. Vitagliano, G. Vecchio, M. Grieco, H4 (D10S170), a gene frequently rearranged with RET in papillary thyroid carcinomas: functional characterization, Oncogene 23 (2004) 109–121.
[34] F. Morra, C. Luise, R. Visconti, S. Staibano, F. Merolla, G. Ilardi, G. Guggino, S. Paladino, D. Sarnataro, R. Franco, R. Monaco, F. Zitomarino, R. Pacelli, G. Monaco, G. Rocco, A. Cerrato, S. Linardopoulos, M.T. Muller, A. Celetti, New therapeutic perspectives in CCDC6 deficient lung cancer cells, Int. J. Cancer 136 (2015) 2146–2157.
[35] F. Morra, C. Luise, F. Merolla, I. Poser, R. Visconti, G. Ilardi, S. Paladino, H. Inuzuka, G. Guggino, R. Monaco, D. Colecchia, G. Monaco, A. Cerrato, M. Chiariello, K. Denning, P.P. Claudio, S. Staibano, A. Celetti, FBXW7 and USP7 regulate CCDC6 turnover during the cell cycle and affect cancer drugs susceptibility in NSCLC, Oncotarget 6 (2015) 12697–12709.
[36] C. Luise, F. Merolla, V. Leone, S. Paladino, D. Sarnataro, A. Fusco, A. Celetti, Identification of sumoylation sites in CCDC6, the first identified RET partner gene in papillary thyroid carcinoma, uncovers a mode of regulating CCDC6 function on CREB1 transcriptional activity, PLoS One 7 (2012) e49298.
[37] V. Leone, C. Langella, F. Esposito, C. Arra, G. Palma, D. Rea, O. Paciello, F. Merolla, D. De Biase, S. Papparella, A. Celetti, A. Fusco, Ccdc6 knock-in mice develop thyroid hyperplasia associated to an enhanced CREB1 activity, Oncotarget. 6 (2015) 15628–15638.
[38] A.R. Kristensen, J. Gsponer, L.J. Foster, A high-throughput approach for measuring temporal changes in the interactome, Nat. Methods 9 (2012) 907–909.
[39] M. Mascolo, G. Ilardi, M.F. Romano, A. Celetti, M. Siano, S. Romano, C. Luise, F. Merolla, A. Rocco, M.L. Vecchione, G. De Rosa, S. Staibano, Overexpression of chromatin assembly factor-1 p60, poly(ADP-ribose) polymerase 1 and nestin predicts metastasizing behaviour of oral cancer, Histopathology 61 (2012) 1089–1105.
[40] P. Bankhead, M.B. Loughrey, J.A. Fernández, Y. Dombrowski, D.G. McArt, P.D. Dunne, S. McQuaid, R.T. Gray, L.J. Murray, H.G. Coleman, J.A. James, M. Salto-Tellez, P.W. Hamilton, QuPath: open source software for digital pathology image analysis, Sci. Rep. 7 (2017) 16878.
[41] D. Russo, F. Merolla, M. Mascolo, G. Ilardi, S. Romano, S. Varricchio, V. Napolitano, A. Celetti, L. Postiglione, P.P. Di Lorenzo, L. Califano, G.O. Dell'Aversana, F. Astarita, M.F. Romano, S. Staibano, FKBP51 immunohistochemical expression: a new prognostic biomarker for OSCC? Int. J. Mol. Sci. 18 (2017) E443.
[42] U.K. Laemli, Cleavage of structural proteins during the assembly of the head of bacteriophage T4, Nature. 227 (1970) 680–685.
[43] H. Towbin, T. Staehelin, J. Gordon, Electrophoretic transfer of proteins from polyacrylamide gels to nitrocellulose sheets: procedure and some applications, Proc. Natl. Acad. Sci. U.S.A. 76 (1979) 4350–4354.
[44] M. Jasin, Genetic manipulation of genomes withrare-cutting endonucleases, Trends Genet. 12 (1996) 224–228.
[45] A.P. Turnbull, S. Ioannidis, W.W. Krajewski, A. Pinto-Fernandez, C. Heride, A.C.L. Martin, L.M. Tonkin, E.C. Townsend, S.M. Buker, D.R. Lancia, J.A. Caravella, A.V. Toms, T.M. Charlton, J. Lahdenranta, E. Wilker, B.C. Follows, N.J. Evans, L. Stead, C. Alli, V.V. Zarayskiy, A.C. Talbot, A.J. Buckmelter, M. Wang, C.L. McKinnon, F. Saab, J.F. McGouran, H. Century, M. Gersch, M.S. Pittman, C.G. Marshall, T.M. Raynham, M. Simcox, L.M.D. Stewart, S.B. McLoughlin, J.A. Escobedo, K.W. Bair, C.J. Dinsmore, T.R. Hammonds, S. Kim, S. Urbé, M.J. Clague, B.M. Kessler, D. Komander, Molecular basis of USP7 inhibition by selective small-molecule inhibitors, Nature 550 (2017) 481–486.
[46] D. Chauhan, Z. Tian, B. Nicholson, K.G. Kumar, B. Zhou, R. Carrasco, J.L. McDermott, C.A. Leach, M. Fulcinniti, M.P. Kodrasov, J. Weinstock, W.D. Kingsbury, T. Hideshima, P.K. Shah, S. Minvielle, M. Altun, B.M. Kessler, R. Orlowski, P. Richardson, N. Munshi, K.C. Anderson, A small molecule inhibitor of ubiquitin-specific protease-7 induces apoptosis in multiple myeloma cells and overcomes bortezomib resistance, Cancer Cell 22 (345) (2012) 58.
[47] U. Malapelle, F. Morra, G. Ilardi, R. Visconti, F. Merolla, A. Cerrato, V. Napolitano, R. Monaco, G. Guggino, G. Monaco, S. Staibano, G. Troncone, A. Celetti, USP7 inhibitors, downregulating CCDC6, sensitize lung neuroendocrine cancer cells to PARP-inhibitor drugs, Lung Cancer 107 (2017) 41–49.
[48] F. Morra, F. Merolla, V. Napolitano, G. Ilardi, C. Miro, S. Paladino, S. Staibano, A. Cerrato, A. Celetti, The combined effect of USP7 inhibitors and PARP inhibitors in hormone-sensitive and castration-resistant prostate cancer cells, Oncotarget 8 (2017) 31815–31829.
[49] F. Morra, F. Merolla, D. Criscuolo, L. Insabato, R. Giannella, G. Ilardi, A. Cerrato, R. Visconti, S. Staibano, A. Celetti, CCDC6 and USP7 expression levels suggest novel treatment options in high-grade urothelial bladder cancer, J. Exp. Clin. Cancer Res. 38 (1) (2019) 90.
[50] G. Srinivasan, G.S. Sidhu, E.A. Williamson, A.S. Jaiswal, N. Najmunnisa, K. Wilcoxen, D. Jones, T.J. George Jr., R. Hromas, Synthetic lethality in malignant pleural mesothelioma with PARP1 inhibition, Cancer Chemother. Pharmacol. 80 (2017) 861–867.
[51] M. Nasu, M. Emi, S. Pastorino, M. Tanji, A. Powers, H. Luk, F. Baumann, Y.A. Zhang, A. Gazdar, S. Kanodia, M. Tiirikainen, E. Flores, G. Gaudino, M.J. Becich, H.I. Pass, H. Yang, M. Carbone, High incidence of somatic BAP1 alterations in sporadic malignant mesothelioma, J. Thorac. Oncol. 10 (2015) 565–576.
[52] B. Evers, R. Drost, E. Schut, M. de Bruin, E. van der Burg, P.W. Derksen, H. Holstege, X. Liu, E. van Drunen, H.B. Beverloo, G.C. Smith, N.M. Martin, A. Lau, M.J. O'Connor, J. Jonkers, Selective inhibition of BRCA2-deficient mammary tumor cell growth by AZD2281 and cisplatin, Clin. Cancer Res. 14 (2008) 3916–3925.
[53] A. Cerrato, F. Morra, A. Celetti, Use of poly ADP-ribose polymerase [PARP] inhibitors in cancer cells bearing DDR defects: the rationale for their inclusion in the clinic, J. Exp. Clin. Cancer Res. 35 (2016) 179.
[54] A. Cerrato, R. Visconti, A. Celetti, The rationale for druggability of CCDC6-tyrosine kinase fusions in lung cancer, Mol. Cancer 17 (2018) 46.
[55] R. Visconti, D. Grieco, Fighting tubulin-targeting anticancer drug toxicity and resistance, Endocr. Relat. Cancer 24 (2017) T107–17.